

Electrochemical characterization of arylene vinylene oligomers containing triphenylamine and carbazole units

Loredana Vacareanu · Mircea Grigoras

Received: 7 August 2009 / Accepted: 4 July 2010 / Published online: 17 July 2010
© Springer Science+Business Media B.V. 2010

Abstract Cyclic voltammetry (CV) has been used to investigate the electrochemical behavior of three arylene vinylene oligomers containing triphenylamine and carbazole units at the ends. The synthesis of oligomers was performed using Wittig reaction conditions, between 4-formyltriphenylamine or 3-formyl-*N*-hexyl-carbazole and two diphosphonium salts. The cyclic voltammograms, recorded in anodic range of potentials, revealed that the oligomers undergo quasi-reversible or irreversible redox processes. Polymer films were deposited on Pt electrode by CV and CPE (Controlled Potential Electrolysis) methods. The polymer films obtained by electrochemical polymerization methods show no solubility in all organic solvents and present similar FT-IR data with those polymers synthesized by chemical oxidative polymerization. Characterizations of the oligomers were made by ¹H-NMR spectroscopy, UV–Vis and fluorescence spectroscopy. Due to the lack of their solubility, the polymers obtained by electrochemical methods were characterized only by FT-IR spectroscopy.

Keywords Arylene vinylene oligomers · Triphenylamine and carbazole derivatives · Cyclic voltammetry · Anodic oxidation · Electrochemical polymerization

1 Introduction

The last years are witness to the development of conjugated arylamine oligomers and polymers as an important class of

electro and photoactive materials, investigated both in academic and industrial laboratories [1–5]. The real interests for conjugated oligomers emerge from interesting application such as active components in organic electronic or electrochemical devices [6, 7]. The advantage of using small conjugated compounds is based on the possibility of tuning their physical properties by changing the chemical structure, e.g., by introduction of side substituent groups, end-capping groups, insertion of certain specific functional groups, and by increasing the oligomer length. Thus, conjugated oligomers are used as model compounds for conducting polymers since their monodispersity, defectless structure, and a better supramolecular organization in the solid state facilitate experimental and theoretical investigations [8].

During the last years, much attention has been paid to triphenylamine (TPA) and carbazole compounds because of their electron donating and hole-transporting properties which can facilitate the charge transport of the electrons and holes, making these compounds promising candidates for photo- and electroluminescence devices [9–12]. It is well known that the central amine nitrogen atom is responsible for this behavior, and thus, arylamines are commonly used as photoconductors in the Xerox process, in laser printers and photocopiers [13–15]. From the structural point of view, carbazole molecules differ from diphenylamines by their planar structure, since it can be further imagined as bonded diphenylamine in *ortho*-positions of phenyl rings, which increase the thermal stability of carbazole-containing materials. When acceptor groups are introduced in the 3- and/or 6-positions, the intercharge transfer is induced. Introduction of vinyl, acetylene, or azomethine moieties in arylamine may lead to new functional materials based on synergistic effect of both of them.

Triphenylamine is a well-known molecule that possesses useful functions such as redox activity, fluorescence,

L. Vacareanu (✉) · M. Grigoras
Department of Electroactive Polymers, “P. Poni” Institute of Macromolecular Chemistry, 41A Gr. Ghica Voda Alley, 700487 Iasi, Romania
e-mail: sloredana@icmpp.ro

ferromagnetism due to the high oxidizability of nitrogen center and hole-transporting properties via radical cation species [16]. Owing to the noncoplanarity of the three phenyl substituent, TPA derivatives can be viewed as 3D systems and the combination with linear π -conjugated systems could be expected to lead to amorphous materials with isotropic optical and charge-transport properties.

Electrochemical behavior is an important part of the optimization process based on investigation of structure–activity relationships. This is due to its redox potentials which may give some ideas about the bonding capability of the compounds to another system via donor–acceptor type interactions. For years, it has been known that energies of the highest occupied (HOMO) and lowest unoccupied (LUMO) levels of a chemical system can be correlated with the corresponding redox potentials, measured by CV in non-aqueous solvents [17, 18]. So, anodic peak potential (E_{ox}) is that potential at which one or more electrons are transferred, preferentially from the HOMO level of the molecule to the anode. This process is called anodic oxidation.

The chemical oxidative polymerization (using FeCl_3) of TPA derivatives like 4-alkyl [19, 20], 4-nitro, or –CN triphenylamine [21], di(1-naphthyl)-4-anilamine [22], and di(1-naphthyl) *p*-tolylamine [23] has been reported. The obtained polymers have relative high molecular weights, are easily soluble in organic solvents, and can be processed in free-standing films with good thermal stability. Therefore, arylamine derivatives having at least one free *para* position for encatennation can be used as monomers in chemical or electrochemical oxidative polymerization.

The aim of this article is to report the synthesis and to describe the electrochemical behavior of three arylenevinylene oligomers based on triphenylamine or *N*-hexylcarbazole units: 1,4-bis [4-(*N,N'*-diphenylamino) phenylvinyl] benzene (**I**), 1,4-bis[4-(*N,N'*-diphenylamino) phenylvinyl] biphenyl (**II**), 3,3'-bis (*N*-hexylcarbazole)vinylbenzene (**III**). As well, we report the electrochemical polymerization of these oligomers and oxidative polymerization reaction of the oligomer **II**. The electronic properties of these new compounds have been analyzed by FT-IR spectroscopy, UV–Vis absorption and fluorescence emission spectroscopy, and cyclic voltammetry (CV).

2 Experimental

2.1 Materials

Triphenylamine, carbazole (Aldrich), and phosphorus oxychloride (Fulka) are commercial products and were used as received. The diphosphonium salts were obtained employing 1,

4-bis (chloromethyl) benzene or 4,4'-bis(chloromethyl) biphenyl (both from Aldrich) and tributyl phosphine. *N,N'*-Dimethylformamide (DMF) and other solvents (all from Aldrich) are commercial products and were used as received or dried by usual methods and distilled under reduced pressure. Tetrabutylammonium tetrafluoroborate (Bu_4NBF_4) was synthesized by neutralization reaction of tetrabutylammonium hydroxide solution (40%) with fluoroboric acid (40% solution) (both from Fluka) and recrystallized twice from ethyl acetate and then dried in vacuo prior to use.

2.2 Instrumentation

The FT-IR spectra were recorded in KBr pellets on a Digilab-FTS 2000 spectrometer, while UV–Vis absorption spectra and fluorescence measurements were carried out in CH_2Cl_2 solution, on a Specord 200 spectrophotometer and Perkin Elmer LS 55 apparatus, respectively. $^1\text{H-NMR}$ spectra were recorded at room temperature on a Bruker Avance DRX-400 spectrometer (400 MHz) as solutions in CDCl_3 , and chemical shifts are reported in ppm and referenced to TMS as the internal standard. Differential scanning calorimetry (DSC) measurements were performed with a Mettler DSC-12E apparatus under nitrogen atmosphere.

The electrochemical studies were carried out with a Bioanalytical System, Potentiostat–Galvanostat (BAS 100B/W). The electrochemical cell was equipped with three electrodes: a working electrode (disk shape, $\Phi = 1.6$ mm), an auxiliary electrode (platinum wire), and a reference electrode (consisted of a silver wire coated with AgCl). In order to obtain sufficient amount of polymers for characterization, a Pt plate with surface area of $1.0 \times 0.5 \text{ cm}^2$ was employed as working electrode. The reference electrode (Ag/Ag^+) was calibrated at the beginning of the experiments by running the CV of ferrocene as the internal standard in an identical cell without any compound in the system ($E_{\text{Fc/Fc}^+} = 0.46 \text{ V}$ versus the Ag/AgCl). Cyclic voltammograms of oligomers were recorded in degassed dichloromethane solution containing tetrabutylammonium tetrafluoroborate (Bu_4NBF_4) as electrolyte. All the measurements were performed at room temperature (about 25 °C) under nitrogen atmosphere.

2.3 Monomers and oligomers synthesis

4-Formyltriphenylamine (**1**) was synthesized by formylation reaction of triphenylamine using POCl_3/DMF reagent, as is described in the literature [24].

N-Hexyl-3-formylcarbazole (**2**) [25] was synthesized by alkylation of carbazole with *n*-hexyl bromide followed by formylation with POCl_3/DMF reagent.

2.3.1 General procedure for Wittig reaction

In a 50-mL two-neck flask, equipped with a magnetic stirrer, 0.204 g (0.375 mmol) of 4-formyltriphenylamine (**1**) and 15 mL of chloroform were added. Then 0.217 g (0.187 mmol) of diphosphonium salt (**3**) or (**4**), dissolved in 15 mL ethanol was added. A solution of sodium ethoxide (9.01 mmol) was freshly prepared and added to the mixture dropwise. The resulting reaction mixture was stirred at room temperature under nitrogen atmosphere for 12 h. The obtained precipitate was filtered off and washed with ethanol. After several purifications by precipitation in methanol from toluene solution, the oligomers were obtained as yellow powders with strong green-yellow fluorescence in diluted solution.

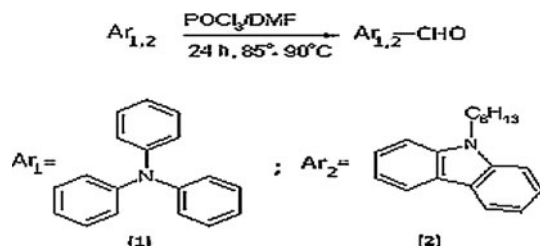
1, 4-bis [4-(*N*, *N'*-diphenylamino)phenylvinyl] benzene (**I**) resulted in 94% yield, and its structure was confirmed by ¹H NMR and FT-IR spectroscopy.

1,4-bis [4-(*N*, *N'*-diphenylamino)phenylvinyl] biphenyl (**II**) resulted in 79% yield according to the procedure reported for **I**, and its structure was confirmed by ¹H NMR and FT-IR spectroscopy.

3, 3'-bis (*N*-hexylcarbazole)vinylbenzene (**III**) was synthesized in the same way as for **I** and **II**. A yellow crystalline powder with 95% yield was obtained.

3 Results and discussions

The synthesis of the intermediates and the target molecules are depicted in the Schemes 1 and 2, respectively. First,



Scheme 1 Monomer synthesis

under Vilsmeier–Haack conditions, the aldehyde group was introduced at 3-position of *N*-hexylcarbazole and *para* position of one phenyl group of triphenylamine molecule (Scheme 1). The small conjugated compounds containing triphenylamine or carbazole at both ends were synthesized under Wittig reaction conditions.

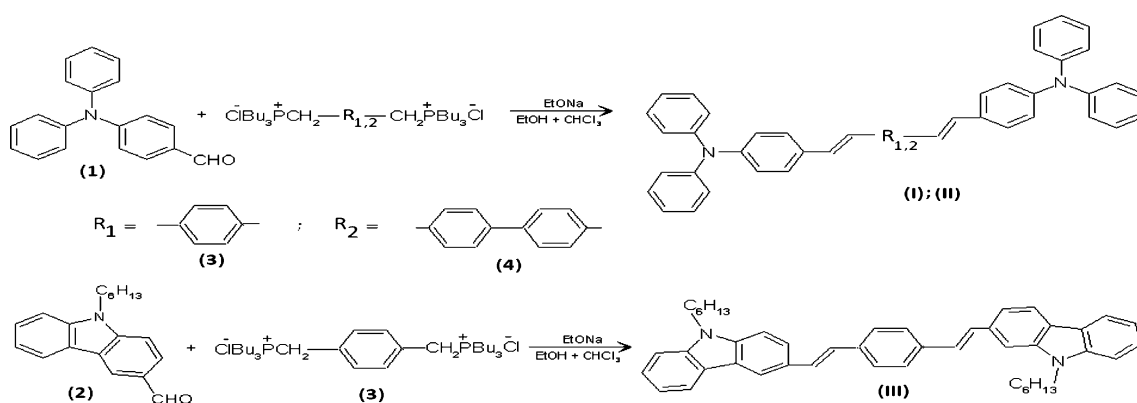
Thus, by coupling 2 mol of monoaldehyde (**1**) or (**2**) with 1 mol of phosphonium salt of 1,4-bis(chloromethyl) benzene (**3**) or 4,4'-bis(chloromethyl)biphenyl (**4**) (Scheme 2) led to 1,4-bis[4-(*N*, *N'*-diphenylamino)phenylvinyl]benzene (**I**), 1,4-bis[4-(*N*, *N'*-diphenylamino)phenylvinyl] biphenyl (**II**) or 3,3'-bis(*N*-hexylcarbazole)vinylbenzene (**III**). These derivatives are oligomers having an arylene vinylene structure with two TPA or carbazole terminal groups.

Having unsubstituted positions (*para*- for **I** and **II** or 3- for **III**), which are active for encatennation, these compounds can be considered as monomers in chemical and electrochemical oxidative polymerization. All compounds were purified by repeated precipitations of toluene solution in methanol to give bright yellow powders with strong fluorescence.

Spectroscopic methods such as FT-IR, ¹H-NMR, UV–Vis, and photoluminescence spectroscopy, were used to identify the structures of these oligomers and the spectroscopic data are summarized in Tables 1 and 2. From the FT-IR data can be observed the characteristic absorption peaks for *trans*-arylene vinylene derivatives.

In the wavelength range from 237 to 600 nm, several absorption peaks appeared, while almost no linear absorption was observed beyond 450 nm. These oligomers have appropriate values of absorption and emission peaks in the case of carbazole oligomer, and the absorption peaks are much broader. The absorption peaks located at 412, 402, and 369 nm can be assigned to electronic π – π^* transition of all conjugated backbone.

The blue shifting of absorption maxima of **II** with respect to **I**, observed in the UV spectra, can be distinguished as well in PL spectra, and this may be explained by the decrease in



Scheme 2 Synthesis of arylenevinylene oligomers based on triphenylamine and carbazole moieties, using Wittig reaction condition

Table 1 ^1H NMR and FT-IR data of oligomers

Oligo- mer	^1H NMR data (δ ppm, CDCl_3)	FT-IR (cm^{-1} , KBr pellets)
I		3023–2920 ($\delta = \text{C}-\text{H}$) 1598, 1492 ($\nu \text{C}-\text{C}$ monosubstituted phenyl) 1589 ($\text{C}=\text{C}$, conjugated phenyl group) 1328 ($\delta \text{C}-\text{N}$ stretching vibration) 960 (out-of-plane bending vibration of $\text{HC}=\text{CH}$ <i>trans</i>) 827 (γCH <i>p</i> -substituted benzene ring) 697–695 ($\delta \text{C}-\text{H}$ phenyl rings)
II		3028–3020 ($\delta = \text{C}-\text{H}$) 1591 ($\nu \text{C}-\text{C}$ monosubstituted phenyl) 1586 ($\text{C}=\text{C}$, conjugated phenyl group) 1316 ($\delta \text{C}-\text{N}$ stretching vibration) 962 (out-of-plane bending vibration of $\text{HC}=\text{CH}$ <i>trans</i>) 821 (γCH <i>p</i> -substituted benzene) 697 – 695 ($\delta \text{C}-\text{H}$ benzene)
III		3435 ($\delta = \text{C}-\text{H}$) 2956, 2856 ($\nu \text{N}-\text{C}$), 1598, 1491, 1477 ($\nu \text{C}-\text{C}$ monosubstituted benzene) 1351 ($=\text{C}-\text{N}$) 962 (out-of-plane bending vibration of $\text{HC}=\text{CH}$ <i>trans</i>) 814 (γCH <i>p</i> -substituted benzene ring) 1154 ($\delta \text{C}-\text{N}$ stretching vibration)

7.469 (s, H_a , 4H), 7.399–7.378 (H_b , d, 4H, $J = 8.4$ Hz), 7.282–7.243 ($\text{H}_c + \text{H}_{d'}$, t, 8H, $J = 8.4$ Hz), 7.123–7.090 (H_d , 8H, $J = 7.6$ Hz), 7.062–6.96 ($\text{H}_e + \text{H}_f$, m, 12H)

7.56–7.844 ($\text{H}_a + \text{H}_b$, dd, 8H, $J = 8.4$ Hz), 7.412–7.39 (H_c , d, 4H, $J = 8.8$ Hz), 7.281–7.242 ($\text{H}_d + \text{H}_{d'}$, d, 8H, $J = 8.0$ Hz), 7.125–7.105 (H_e , d, 8H, $J = 8.0$ Hz), 7.083–7.004 ($\text{H}_f + \text{H}_g$, m, 12H).

8.26 (1H, H_j), 7.69 (1H, H_d , $J = 8.4$ Hz), 8.16 (1H, H_i), 7.50 (1H, H_h), 7.42 (1H, H_l), 7.38 (1H, H_e), 7.23 (1H, H_g), 7.36 and 7.18 (2H, H_c and $\text{H}_{b'}$), 7.58 (4H, H_a), 4.28 (2H, $- \text{N}-\text{CH}_2$), 1.88 (2H, $-\text{CH}_2-$), 1.31–1.43 (6H, $-(\text{CH}_2)_3$), 0.89 (3H, t, $-\text{CH}_3$)

conjugation length due to noncoplanarity of **II**. From the point of view of light-emitting material applications, this behavior of **II** can be considered an advantage because the electroluminescent materials have to be thermally stable, to present a low tendency for aggregation and excimer formation, crystallization, and destruction. The carbazole derivatives exhibit a blue-yellow fluorescence in methylene chloride solution, and the triphenylamine compounds have a green-yellow fluorescence.

Increasing the molecular weight should increase the glass-transition temperature, and the DSC analysis of the oligomers confirms this affirmation. The DSC curves were recorded at a heating rate of 15 °C/min from 20 °C (initial temperature) to 280 °C (final temperature) (Fig. 1). In the first scan, in the case of all oligomers, the DSC measurements revealed endothermic peaks associated with melting process. For derivative **I**, an endothermic peak can be

Table 2 Optical data for oligomers

Oligomer	$\lambda_{\text{abs}}^{\text{max}}$ (nm) ^a	$\lambda_{\text{em}}^{\text{max}}$ (nm) ^a	E_g (eV) ^b
I	310; 412	472	2.68
II	308; 402	465	2.75
III	244; 310; 396	472	2.78

^a Measured in diluted CH_2Cl_2 solution

^b Obtained from UV–Vis spectra: $E_g = 1240/\lambda_{\text{onset}}$

observed at 212 °C, which can be assigned to the melting process. The isotropic liquid was then quickly cooled when an amorphous glass is formed. In the DSC curve, during the second heating scan the glass-transition process (T_g) can be observed. This is located at 85 °C, followed by a crystallization process, and the melting temperature peak appeared at 210 °C.

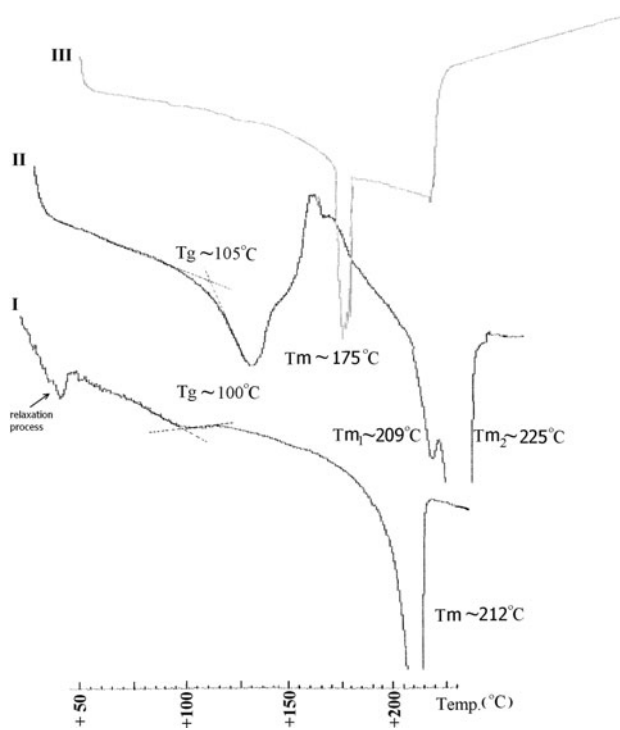


Fig. 1 Thermal behavior of oligomers (the first heating run), determined by DSC analysis

Oligomer **II** exhibits two melting temperature peaks located at $T_{m1} = 209\text{ }^{\circ}\text{C}$ and $T_{m2} = 225\text{ }^{\circ}\text{C}$, probably due to two crystalline states being present. The crystallization temperature is situated at $155\text{ }^{\circ}\text{C}$. In the second scan, the T_g was observed at $105\text{ }^{\circ}\text{C}$, but the melting process disappeared due to the oligomer not being crystallized after cooling and remaining in an amorphous state. The absence of the crystallization process can be explained from the structural point of view. The two phenyl rings from the biphenyl central unit of **II** are twisted with a dihedral angle to one another due to sterical hindrances between *ortho*-hydrogen atoms. The non-planarity of the molecule explains why crystallization is a very low-rate process and the formation of glass state by cooling. Therefore, the oligomer **II** can be used in vacuum deposition technique for processing it into thin films for OLED applications due to its slow rate of crystallization process. Carbazole oligomer (**III**) exhibits a crystallization process at $115\text{ }^{\circ}\text{C}$ and a melting process, $T_m = 170\text{ }^{\circ}\text{C}$. These results show that these compounds are not stable at higher temperature.

3.1 Electrochemical studies

In addition to thermal stability and the ability to form amorphous films, the electrochemical stability is another condition to be fulfilled by electroactive materials in order

to find applications in various electro-optical devices. CV is a very useful method which reveals the electron transfer during the electropolymerization and also examines the electroactivity of the polymer films. The oxidation and reduction process can be monitored in form of a current–potential diagram [26]. We applied this method for all three oligomers, and the CVs were recorded in the anodic potential range between 0.0 and 1.8 V. No oxidation was seen on the anodic scan up to a potential of 1.8 V. All the CVs were recorded maintaining the same conditions: solvent, scan rate, concentration of the monomers and salt, and anodic potential range.

In Fig. 2, the CVs of **I** are presented in methylene chloride solution, obtained during the successive scans between 0.0 and 1.8 V versus Ag/AgCl. On the first anodic scan, two oxidation peaks can be clearly distinguished at $E_{ox1} = 0.88\text{ V}$ and $E_{ox2} = 1.08\text{ V}$ and two reduction peaks located at $E_{red1} = 0.94\text{ V}$ and $E_{red2} = 0.77\text{ V}$.

The CVs are quasi-reversible, and oxidation peaks are associated with the loss of two electrons obtaining unstable cation radicals. In the next steps, these cation radicals react either with other cation radicals or with neutral parent molecule. In the CVs of **I**, two cathodic peaks can be assigned to the reduction of the oxidized species presented in the solution. During the repetitive scanning of CVs of compound **I** in the range 0.0 V–1.8 V, the first oxidation peak (E_{ox1}) disappears with increasing the number of scans and the potential value for the second one (E_{ox2}) is slightly shifted in the positive direction. The same thing happened with the reduction peaks, but the values of these peaks are slightly shifted in the negative direction. In both cases, the intensity of the current increases with the number of scans; this indicates that a new electroactive structure is formed and deposited on working electrode. Such a behavior has

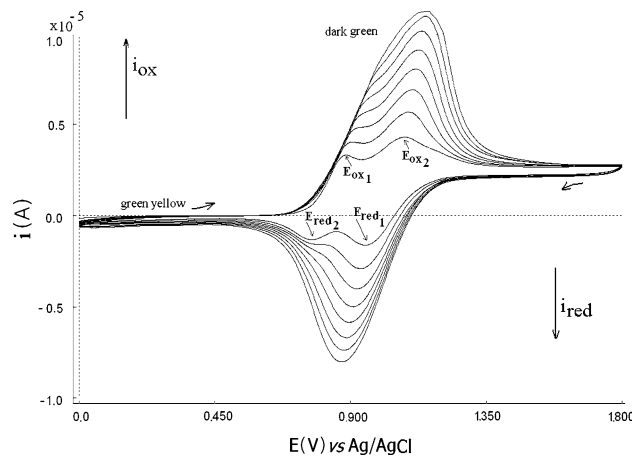


Fig. 2 Cyclic voltammograms for 1,4-bis[4-(*N,N'*diphenylamino)phenylvinyl]benzene (**I**), $2 \times 10^{-3}\text{ M}$, using Bu_4NBF_4 , as support electrolyte, $2 \times 10^{-1}\text{ M}$. Scan rate: 50 mV s^{-1} between 0.0 and 1.8 V versus Ag/AgCl

already been described by Ambrose and Nelson [27] during the anodic oxidation of *N*-ethylcarbazole in solution, which corresponds to the formation of the 3,3'-dimer. Finally, at a higher number of scans, only one oxidation peak appears, which is shifted to more positive potential values. Therefore, during the oxidation processes of oligomer **I**, a green color polymer film is formed on the platinum electrode surface. The oligomer **II** exhibits three oxidation peaks and one detectable reduction peak on the reverse scanning (Fig. 3).

In general, increasing the chain length involves a higher electronic delocalization which may cause differences in redox behavior of the derivatives. Thus, in the case of oligomer **II** having two phenyl rings, we expect to present different anodic and cathodic behavior than oligomer **I**. Therefore, the CVs (recorded vs Ag/AgCl) of oligomer **II**, three anodic peaks can be observed at $E_{\text{ox}1} = 0.96$ V, $E_{\text{ox}2} = 1.04$ V, and $E_{\text{ox}3} = 1.25$ V, and on the reverse scanning, only one reduction peak was observed at $E_{\text{red}} = 0.96$ V.

The oxidation peaks are very broad and do not have a well-defined shape. This may be caused by introducing the biphenyl into the arylene vinylene structure, which increased the π -conjugation length. The first two oxidation peaks are irreversible. By increasing the number of scans, only one oxidation peak appears and the peak potential values are slightly shifted in the positive direction. By scanning in the opposite direction the values of the reduction peak are shifted in negative direction with increasing the number of scans. In both cases the intensity of the peak current increased regularly during the successive scans (Fig. 3). Finally, we obtained a green-dark polymer film deposited on the Pt plate electrode.

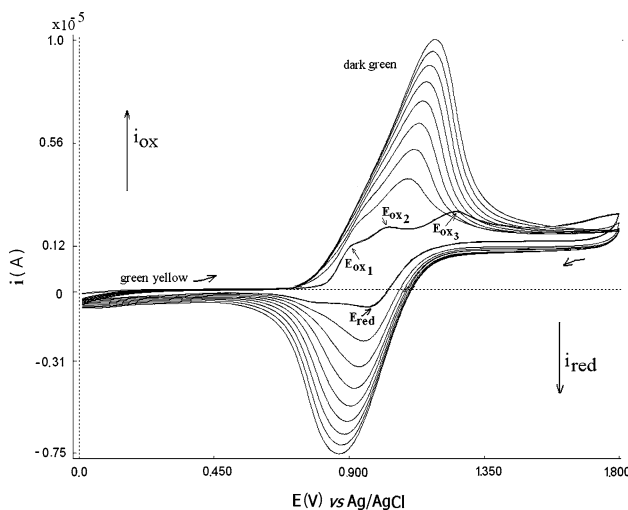


Fig. 3 Cyclic voltammograms for 1,4-bis[4-(*N,N'*-diphenylamino)phenylvinyl] biphenyl (**II**), 2×10^{-3} M, using Bu_4NBF_4 , as support electrolyte, 2×10^{-1} M. Scan rate: 50 mV s^{-1} between 0.0 and 1.8 V versus Ag/AgCl

The carbazole oligomer (**III**) exhibits irreversible CVs, presented in Fig. 4. The first scan (dotted line) revealed three oxidation peaks and two reduction peaks. First oxidation peak, occurring at $E_{\text{ox}1} = 0.82$ V, is irreversible and is caused by the formation of the cation radical which follows the typical ECE mechanism, like triphenylamine derivatives. The further oxidation process revealed two anodic peaks at $E_{\text{ox}2} = 1.03$ V and $E_{\text{ox}3} = 1.49$ V. This can be attributed to the dimerization process. On the reverse scanning, two reduction peaks can be observed located at $E_{\text{red}1} = 1.26$ V and $E_{\text{red}2} = 0.90$ V, which are very broad.

Recording the CVs by running a higher number of scans, the oxidation peaks are shifted to more positive potentials. It can be observed that the intensity of these peaks decreases with increasing the number of scans. Finally, at the 15th scanning, some of the peaks disappeared and two new oxidation peaks appear at 1.04 and 1.56 V. No polymeric film was obtained on Pt plate electrode by recording a repetitive CVs scanning. This can be explained by the presence of the C_6H_{13} substituent attached at the nitrogen atom of carbazole units, which confers to the obtained polymer a good solubility in methylene chloride.

According to the correlation which can be done, between HOMO and LUMO energy levels and redox potentials, the value of the energy levels can be calculated from CVs using the onset values of the oxidation and reduction peaks. The onset values are estimated from the intersection of the two tangents drawn at the rising oxidation (or reduction) current and the background current in the CVs. According to Li et al. [28], the E^0 of the redox couple Fc/Fc^+ , measured in Bu_4NBF_4 methylene chloride solution, is equal to 0.46 V versus Ag/AgCl, and

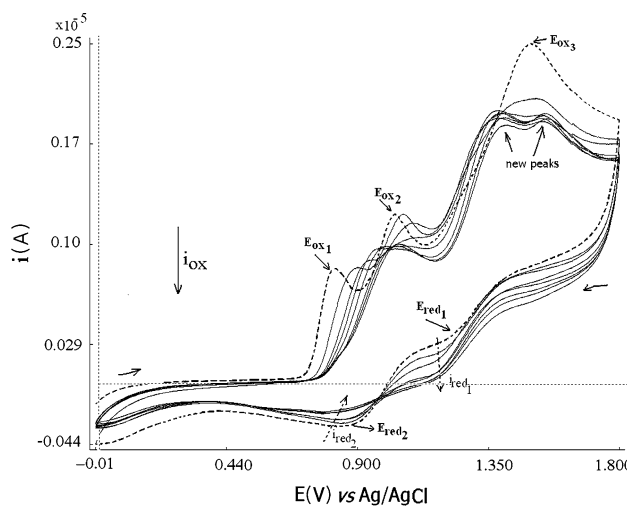


Fig. 4 Cyclic voltammograms for 3,3'-bis(*N*-hexylcarbazole)vinylbenzene (**III**), 2×10^{-3} M, using Bu_4NBF_4 , as support electrolyte, 2×10^{-1} M. Scan rate: 50 mV s^{-1} between 0.0 and 1.8 V versus Ag/AgCl

Table 3 Electrochemical characteristics of oligomers

Oligomer	$E_{\text{ox}}^{\text{onset}}$ (V) versus Ag/AgCl	$E_{\text{red}}^{\text{onset}}$ (V) versus Ag/AgCl	E_{HOMO} (e V)	E_{LUMO} (e V)	E_g^{a} (e V)	$i_{\text{red}}/i_{\text{ox}}^{\text{b}}$
I	0.74	1.13	-5.08	-3.21	1.87	0.49
II	0.80	1.12	-5.14	-3.22	1.92	0.32
III	0.72	1.39	-5.06	-2.95	2.11	0.15

^a $E_g = E_{\text{HOMO}} - E_{\text{LUMO}}$

^b $i_{\text{red}}/i_{\text{ox}}$ = the peak current ratio

the energy levels of oligomers (in electron volts, eV) can be obtained by adding 4.34 V to the values of the redox potential. Thus, $E_{\text{HOMO}} = -e(E_{\text{ox}}^{\text{onset}} + 4.34)$ and $E_{\text{LUMO}} = -e(E_{\text{red}}^{\text{onset}} + 4.34)$. The electrochemical data are summarized in the Table 3.

According to their theoretical calculations, Wang et al. [29] suggested that the central amine nitrogen atom is the major contributor to the HOMO energy level, and the phenyl rings, which are around the amine nitrogen atom, are the major contributor for LUMO energy level. Therefore, the values of both HOMO and LUMO energy levels can be affected by the substituent of triphenylamine and carbazole oligomers. Oligomer **II** has a biphenyl central unit, which is not located in the same plane and is twisted forming a dihedral angle between the two phenyl rings. This may lead to an interruption of the π -conjugation of the system that may cause a decrease in the HOMO energy level value than for the other two oligomers. The lower values of HOMO energy levels for oligomers **III** and **I** suggest that these compounds possess a better hole-injecting/transport capability compared to oligomer **II**. Also, the orbital energy of LUMO decreases with an increase in the number of phenyl units between two amine nitrogen atoms.

It is well known that for reversible process yields, a peak current ratio is, $i_{\text{red}}/i_{\text{ox}}$, equal to 1. From the data of these experiments, the values of the peak current ration are less than 1. Thus, we can say that the oligomer **I** undergoes a quasi-reversible redox process and for the other two oligomers the redox process are irreversible.

3.2 Electrochemical polymerization

To obtain a large amount of polymer for characterizations, we used a platinum plate with 0.5 cm^2 area and the same experimental conditions, like in CV. The method that we applied is Controlled Potential Electrolysis which consists of maintaining a constant value for oxidation potential during a precise time. The obtained polymer films are insoluble in all solvents, and its structure could be analyzed only by FT-IR spectroscopy.

The anodic oxidation of triphenylamine and its derivatives was extensively studied starting from 1966 [30–34]. As a conclusion of these studies, these oligomers fall in the

category of multi-step processes involving electrochemical-chemical-electrochemical (ECE) reactions. In the first step a cation radical is formed ($\text{TPA}^{\bullet+}$) by oxidation and this is not stable and dimerizes to tetraphenylbenzidine. If all phenyl groups of TPA derivative are tri-*para*-substituted, the only reaction is the reversible one-electron transfer. In our case, both derivatives of triphenylamine, **I** and **II**, have two free *para* positions at every end. Therefore, their cation radicals are unstable and could dimerize to form tetraphenylbenzidine derivatives, and all process can be continued until polymer films are deposited on electrode surface or at the bottom of electrochemical cell.

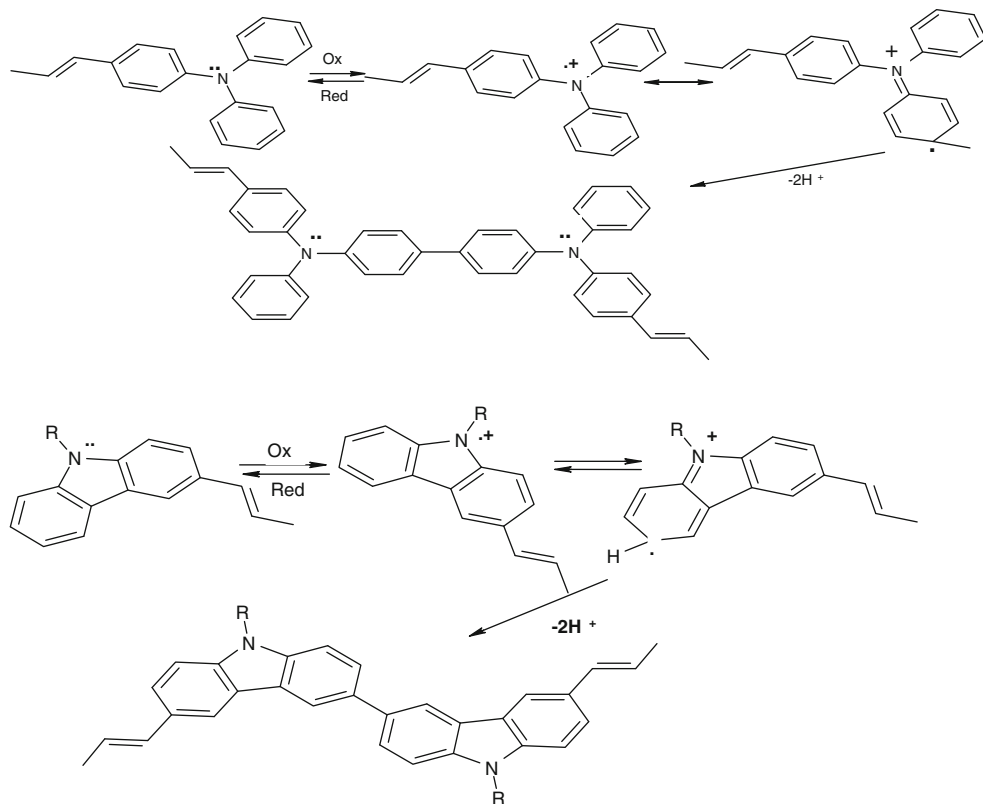
The reaction mechanism for oxidative polymerization of arylenevinylene oligomers is presented in Scheme 3.

The carbazole ring submitted to a positive potential in an electrochemical cell is known to be oxidized to an unstable cation radical. This disappears by coupling at the 3-position with another cation radical when two protons are released [35].

4 Conclusions

Nitrogen-containing heterocycles are of special interest because they form an important class of natural and non-natural products, many of which exhibit useful biological activities and unique electrical and optical properties. To be candidates for the use in hole-transporting layers, organic materials should possess properties such as good electrochemical stability, a low ionization potential, reversible redox behavior, and hole-transporting and hole-injection ability. In addition, thermal and photo stability and good film-forming properties are required. However, these oligomers suffer from low thermal stability due to their low glass-transition temperatures.

Cyclic voltammetry was carried out in order to obtain information about the electrochemical stability and the reversibility of the redox process of oligomers. All three oligomers exhibit redox activity in the range of potential 0.0–1.8 V. All CVs were recorded using a three-cell electrode, and the values of the redox peaks were measured versus Ag/AgCl. Up to 1.8 V the oligomers do not suffer any oxidation or reduction reactions. By increasing the π -conjugation length which implies a higher electronic



Scheme 3 Possible mechanism for (electro) chemical oxidative polymerization of arylenevinylene oligomers

delocalization, the redox behavior of the compound is changing. The gap energy calculated using the CVs data, showed that the oligomer **II** exhibited a slightly lower value of E_g than that of the other two oligomers. CVs data showed that these oligomers undergo quasi-reversible or irreversible redox process which gives us interesting data about the stability of the cation radicals that are formed during the process. After recording several CVs we obtained a dark green polymeric film which is not soluble in any organic solvents. Knowing the redox and chemical data, the highest occupied (HOMO) and lowest unoccupied (LUMO) energy levels of chemical systems can be easily modified to lead to new and improved hole-transporting materials. From the onset potentials of both oxidation and reduction and using the classical equations, the LUMO and HOMO energy were calculated.

Acknowledgments The authors thank to the Romanian National Authority for Scientific Research (UEFISCSU) for financial support (project number 649/2009, PN II- IDEI 993/2008).

References

1. Skotheim TA, Reynolds JR (eds) (2007) Handbook of conducting polymers, 3rd edn. CRC Press, Boca Raton
2. MacDiarmid AG (2001) Angew Chem Int Ed 40:2581
3. Heeger AJ (2001) Angew Chem Int Ed 40:2591
4. Heinze J (1990) Top Curr Chem 152:1
5. Higgins SJ (1997) Chem Soc Rev 26:247
6. Noda T, Ogawa H, Noma N, Shirota Y (1999) J Mater Chem 9:2177
7. Otsubo T, Aso Y, Takimiya K (2002) J Mater Chem 12:2565
8. Nakanishi H, Aso Y, Otsubo T (1999) Synth Met 101:604
9. Kim DY, Cho HN, Kim C (2000) Prog Polym Sci 25:1087
10. Tabata M, Fukushima T, Sadahiro Y (2004) Macromolecules 37:4342
11. Sanda F, Nakai T, Kobayashi N, Masuda T (2004) Macromolecules 37:2703
12. Tang BZ, Chen HZ, Xu RS, Lam JYW, Cheuk KKL, Wong HNC, Wang M (2000) Chem Mater 12:213
13. Stolka M, Yanus JF, Pai DM (1984) J Phys Chem 88:4707
14. Thelakkat R, Fink R, Haubner F, Schmidt HW (1997) Macromol Symp 125:157
15. Thelakkat M (2002) Macromol Mater Eng 287:442
16. Bernius MT, Inbasekaran M, O'Brien J, Wu WS (2000) Adv Mater 12:1737
17. Akbulut U, Toppore L, Türker L (1985) J Polym Sci Polym Chem Ed 23:1631
18. Akbulut U, Toppore L, Türker L (1983) Macromol Chem 184:1661
19. Sim JH, Yamada K, Lee SH, Yokokura S, Sato H (2007) Synth Met 157:940
20. Ogino K, Kanegae A, Yamaguchi R, Sato H, Kurjata J (1999) Macromol Rapid Commun 20:103
21. Lin HY, Liou GS (2009) J Polym Sci A Polym Chem 47:285
22. Lin HY, Liou GS, Lee WY, Chen WC (2007) J Polym Sci A Polym Chem 45:1727
23. Nomura M, Shibasaki Y, Ueda M, Tugita K, Ichikawa M, Taniguchi Y (2004) Macromolecules 37:1204
24. Grigoras M, Vacareanu L (2009) Des Mon Polym 1:21

25. Grigoras M, Antonoaia NC (2005) *Polym Int* 54:1641
26. Xie Y, Jiang F, Xu J, Zeng L, Dong B, Fan C, Zhao F (2009) *Synth Met* 159:298
27. Ambroso JF, Nelson RF (1968) *J Electroanal Soc* 115:1159
28. Li Y, Cao Y, Gao J, Wang D, Yu G, Heeger A (1999) *Synth Met* 99:243
29. Wang BC, Liao HR, Chang JC, Chen L, Yeh JT (2007) *J Lumin* 124:333
30. Seo ET, Nelson RF, Fritsch JM, Marcoux LS, Leedy DW, Adams RN (1966) *J Am Chem Soc* 88:3498
31. Marcoux LS, Adams RN, Feldberg SW (1969) *J Phys Chem* 73:2611
32. Creason SC, Wheeler J, Nelson RF (1972) *J Org Chem* 37:4440
33. Chiu KY, Su TX, Li JH, Lin TH, Liou GS, Cheng SH (2005) *J Electroanal Chem* 575:95
34. Faber R, Mielke GF, Rapta P, Stasko A, Nuyken O (2000) *Coll Czech Chem Commun* 65:1403
35. Simionescu CI, Ivanoiu MG, Grigoras M (1986) *Eur Polym J* 22:71